SI Appendix

Fig. 1. Time dependence of the number of water molecules *N(t)* in the confined space between the melittin surfaces. We only consider the volume at the center of the melittin surfaces where cavitation occurs (indicated by the yellow circle in Fig. 4*a*). A few examples at different pressures and separations are shown.

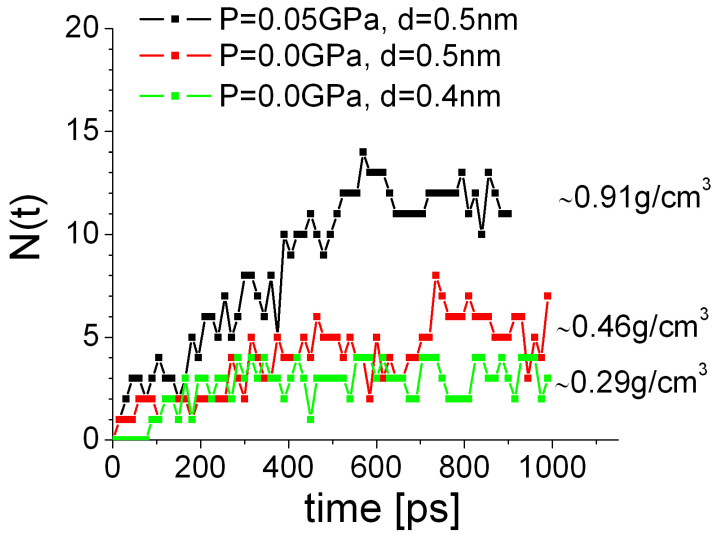

In the examples shown, we run simulations with dry initial conditions. At approximately t = 500ps, the density stabilizes and reaches a constant value. The corresponding final densities are indicated in the figure.

At P = 0GPa and d = 0.4, 0.5 nm, the final density is low (<0.6 g/cm^3) indicating that cavitation occurs. At P = 0.5 GPa and d = 0.5 nm, water remains in the liquid phase.

Fig. 2. Average density of water confined by melittin surfaces for different pressures at d = 0.8nm. This figure is analogous to Fig. 5, which shows data from simulations at d = 1.6 nm. Blue, green, and black lines correspond to water confined by hydrophilic (1) , melittin (this work), and hydrophobic (1) surfaces, respectively. Red line corresponds to bulk water from ref. 2.

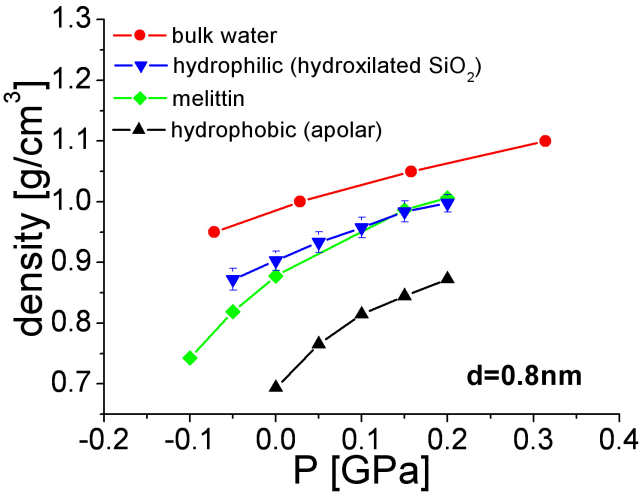

At both separations, d = 0.8 and 1.6nm, the density and compressibility of water confined by the melittin surfaces are closer to those of water confined by the hydrophilic surfaces. The similarities are more pronounced at d = 0.8 nm.

Fig. 3. (*a*) Water density profile ρ(*z*) at different pressures. The separation between the surfaces is *d* =1.6nm. The values of *z* where the density profile is zero correspond to the location of the two melittin dimers. (*b*) Average coordination number CN for water molecules in slabs of width $\delta z = 0.0411$nm located at *z*. All oxygen atoms in the melittin surfaces are considered in the calculations.

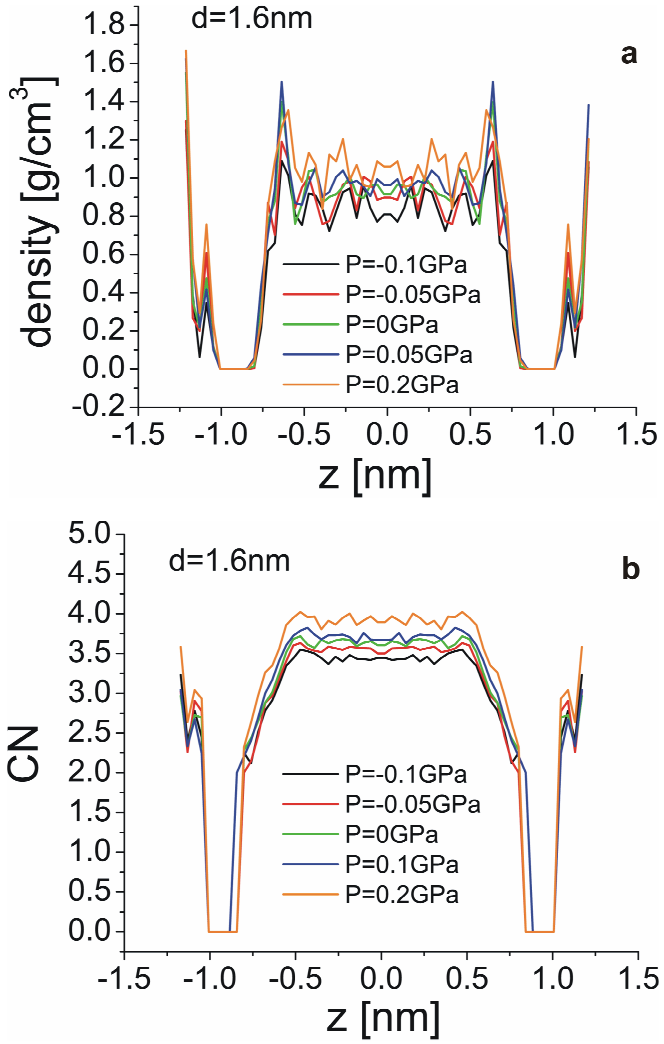

Methods

The initial structure used is the crystal structure of the Melittin dimer (3) from the protein data bank (PDB ID: 2MLT). Hydrogen atoms were added to the X-ray coordinates using the *psfgen* utility contained in the VMD molecular visualization and manipulation package (4) and using the default atom parameter values from the CHARMM v27 force field. This force field was also chosen for the representation of the individual atomic parameters (5). The CHARMM force field has been used for several years and is one of those accepted in mimicking the bonding and non-bonded properties of biomolecular systems. The individual atoms are described by the charges dictated by the CHARMM v27 force field, except as described specifically above. When Leu^{13} is replaced with Asn^{13} (L13N) in each monomer, we find a small gap embedded in the protein interface in the center of the surface due to the slightly smaller radius of the atoms composing the Asn residue. To alleviate any remote possibility of an impact from the presence of this gap in the surface, an atom with no connectivity was fixed within the gap. The extra atom has the non-bond parameters of the alkane carbon CT1 in the CHARMM v27 force field and is uncharged.

We perform molecular dynamics (MD) simulations of a system composed of N = 3,375 water molecules in a cubic box where we immerse two flattened and truncated melittin dimers. The melittin dimers are immobile and the separation between them, defined as the distance between the planes containing the outermost atoms of the flat surfaces, is in the range $0.4 \leq d \leq 1.6$ nm. The simulations are performed at T = 300 K and P = - 0.05 to 0.2 GPa.

We use periodic boundary conditions along the three dimensions. The melittin dimers are located symmetrically about the center of the box, perpendicular to the *z*-axis, such that their flat surfaces face each other (see Fig. 6). The dimers are rotated with respect to each other as observed in the melittin crystal structure (see Fig. 1). The melittin dimer's flat surface dimensions are roughly 1.4 x 2 nm^2, while the linear dimension of the primarily solvent-filled simulation cell changes with P but is always larger than 4.75nm. The present simulations are similar to those reported in refs. 1 and 6 where the two silica-based structured walls implemented in those studies are replaced by melittin dimers. The surface dimensions of the walls used in refs. 1 and 6 are 3.21 x 3.21 nm^2; hence, the melittin dimer's surface is approximately 40% smaller than that of the walls of refs. 1 and 6.

Water molecules are represented by the extended simple-point-charge (SPC/E) model (7) and long-range interactions are treated by using the Ewald sum method (8, 9). We control the temperature using a Berendsen thermostat (10) , and the pressure is controlled by coupling the system to an external bath at P (analogous to the Berendsen thermostat). The pressure is obtained from the virial expression for a three-dimensional system taking into account that the melittin surface atoms are fixed (i.e., by leaving out virial contributions between fixed atom pairs). We have used the same technique in ref. 1 to calculate the pressure.

In general, we start the simulations with water molecules filling the confined space (i.e., wetted initial condition). Only at $d \leq 0.5$ nm and at ($P = 0$; $d \leq 0.9$ nm) we start the simulations with a dry confined space as the initial condition, since the space available to any solvent in these cases is sterically hindered. The simulation times (see

Table 1) are long enough and the initial condition should not affect the results. For example, at the smaller separations, d=0.4-0.5nm, we find that the average number of water molecules in the confined space reaches a constant value after ~500 ps. This is in agreement with the simulations of ref. 11, where cavitation between melittin surfaces is observed to occur after ~400ps. For larger values of d or P, we find that the average number of water molecules in the confined space reaches a constant value at shorter times. The production runs utilized here are summarized in Table I. All depictions of the melittin molecules were visualized using the VMD program (4).

Table 1. Total simulation times for the state points indicted in Fig. 3. Pressures are given in parentheses.

d [nm]	Simulation time, ps*
≥1.0	300 (≤ 0.2 GPa)
0.9-0.7	1000 (≤ 0.2 GPa)
0.6	600 (-0.05 GPa); 1000 (0 GPa); 850 (0.05 GPa); 300 (0.2 GPa)
0.5	1000 (0 GPa); 900 (0.05 GPa)
0.4	1000 (0 GPa)

*If bulk cavitation occurs, the simulation is stopped before the total simulation time is reached. These runs are not listed in the table.

1. Giovambattista N, Rossky PJ, Debenedetti PG (2006) *Phys Rev E* 73:041604/1-041604/14.
2. Starr FW, Sciortino F, Stanley HE (1999) *Phys Rev E* 60:6757-6768. For a better comparison with our results, the values of P taken from this work have been corrected so Lennard-Jones corrections are eliminated (see ref. 1).
3. Terwilliger TC, Eisenberg D (1982) *J Biol Chem* 257:6010-6015.
4. Humphrey W, Dalke A, Schulten K (1996) *J Mol Graphics* 14.1:33-38.
5. MacKerell AD, Bashford D, Bellott M, Dunbrack RL, Evanseck JD, Field MJ, Fischer S, Gao J, Guo H, Ha S, Joseph-McCarthy D, Kuchnir L, Kuczera K, Lau FTK, Mattos C, Michnick S, Ngo T, Nguyen DT, Prodhom B, Reiher WE, Roux B, Schlenkrich M, Smith JC, Stote R, Straub J, Watanabe M, Wiórkiewicz-Kuczera J, Yin D, Karplus M (1998) *J Phys Chem B* 102:3586-3616.
6. Giovambattista N, Debenedetti PG, Rossky PJ (2007) *J Chem Phys C* 111:1323-1332.
7. Berendsen HJC, Grigera JR, Straatsma TP (1987) *J Phys Chem* 91:6269-6271.
8. Nymand TM, Linse P (2000) *J Chem Phys* 112:6152-6160.

9. Toukmaji AY, Board JA, Jr (1996) *Comput Phys Commun* 95:73-92.
10. Berendsen HJC, Potsma JPM, van Gunsteren WF, Di Nola A, Haak JR (1984) *J Chem Phys* 81:3684-3690.
11. Liu P, Huang X, Zhou R, Berne BJ (2005) *Nature* 437:159-162.